phys. stat. sol. (b) **153**, 641 (1989)

Subject classification: 71.35 and 78.55; S8.15

Groupe de Physique des Solides de l'Ecole Normale Supérierure, associe au C.N.R.S., U.A. 17, Université Paris 7[1]

Exciton Transfer between Localized States in $CdS_{1-x}Se_x$ Alloys

By

C. Gourdon and P. Lavallard

Picosecond time resolved luminescence is investigated of excitons localized by alloy potential fluctuations in $CdS_{1-x}Se_x$. Time resolved luminescence spectra, as well as time decay curves and time integrated luminescence spectra of a $CdS_{0.36}Se_{0.64}$ sample are fitted using a model in which transfer to lower energy states occurs through the tunnel effect assisted by acoustic phonons. The density of states is taken to be exponential with a characteristic energy, E_0, equal to 2.2 meV. The radiative lifetime is 1.5 ns. The nonradiative lifetime due to transfer is inversely proportional to the number of available states at lower energy. Close agreement with the experimental results can also be found with a phenomenological model.

Nous étudions la luminescence résolue en temps due aux excitons localisés par les fluctuations de potential d'alliage dans $CdS_{1-x}Se_x$. Les spectres de luminescence résolue en temps, les courbes de décroissance temporelle ainsi que les spectres de luminescence intégrée en temps d'un échantillon de composition $CdS_{0,36}Se_{0,64}$ sont ajustés en utilisant le modéle de transfert par effet tunnel assisté par phonon acoustique. La densité d'états décroit exponentiellement avec une énergie caractéristique $E_0 = 2{,}2$ meV. Le temps de vie radiatif est égal à 1,5 ns. Le temps de vie non-radiatif dû au transfert est inversement proportionnel au nombre d'états disponibles à plus basse énergie. Un modèle phénoménologique donne également un bon accord avec les résultats expérimentaux.

1. Introduction

In the virtual crystal approximation semiconductor solid solutions are described as crystals with intermediate properties between those of the parent binary compounds, i.e. a mean lattice constant and an intermediate band gap energy. Beyond this approximation, disorder effects due to the random distribution of substitutional atoms are responsible for the localization of excitons. This brings about a substantial modification of the optical properties of mixed crystals at low temperature. Among II–VI semiconductor compounds, $CdS_{1-x}Se_x$ has proved to be a good model system for the study of exciton localization due to alloy potential fluctuations [1]. Time integrated luminescence (TIL) was thoroughly investigated by Cohen and Sturge [2] and Permogorov et al. [3]. Experimental time resolved luminescence (TRL) results were reported by several groups including ourselves in the nanosecond and picosecond time range [4 to 8]. We report here on TRL in $CdS_{0.36}Se_{0.64}$. Luminescence decay curves, time resolved spectra, and time integrated spectra are fitted using three theoretical models.

In $CdS_{1-x}Se_x$, for compositions between a few percent and 70%, luminescence spectra consist of a broad and intense luminescence band and its LO phonon replica. From its spectral position, as a function of composition and temperature, and its polarization, this band was attributed to the radiative recombination of localized excitons (LE) [2, 3]. Further evidence for localized excitons was given by the observation of laser narrowing in the LO phonon replica when the laser is tuned to a photon energy inside the broad luminescence band. TRL results demonstrated that spectral

---

[1] Tour 23-2, Place Jussieu, F-75251 Paris Cédex 05, France.

diffusion occurs in the LE band [5 to 8]. The maximum of the luminescence spectrum shifts to lower photon energies with increasing delay after a pulsed excitation. Both rise and decay times of the luminescence signal increase with decreasing observation photon energy in the LE band. In order to explain the shape of the LE luminescence band under selective excitation at low temperature Cohen and Sturge proposed the following description [2]: the excitons created by selective excitation in a localized state, at some definitive energy, transfer to lower-energy localized states by the tunnel effect assisted by acoustic phonons. In principle both spectral and spatial diffusion are taken into account in this model. Energy conservation is assured through exciton–phonon interaction. Spatial transfer can occur owing to the overlap of localized exciton wave functions. However, for the sake of simplicity, spatial position and energy are assumed to be uncorrelated and the spatial dependence of the transfer probability disappears through integration over space.

The authors, however, have only fitted TIL spectra with their model in a very specific situation: when the radiative lifetime is much longer than the nonradiative lifetime due to the transfer process and under the assumption that this nonradiative time is approximately independent of photon energy. This means that the selective excitation lies on the low-energy side of the LE band. We extend here their calculations by explicitly taking into account the energy dependence of the nonradiative transfer rate.

In Section 2 experimental results on TIL and TRL spectra are presented. Theoretical fits are carried out. The fitting parameters are the radiative lifetime, the specific energy for which the transfer rate becomes equal to the radiative one, and the characteristic energy describing the energy dependence of the density of states. The approximations involved in the model are discussed in Section 3. Comparison with two other models is presented in Section 4.

2. Theoretical and Experimental Results

2.1 Theory

The time evolution of the energy dependent excitonic density $n(E, t)$ is described by the usual rate equation

$$\frac{\mathrm{d}n(E,t)}{\mathrm{d}t} = -\frac{n(E,t)}{T(E)} - \sum_{E'<E} W(E \to E')\, n(E,t) + \sum_{E'>E} W(E' \to E)\, n(E',t)\,, \tag{1}$$

where $W(E \to E')$ is the transfer rate from energy E to E' and $T(E)$ is the lifetime due to radiative decay and, eventually, to nonradiative decay processes other than transfer.

At low temperature we only consider transfer to lower energy states. The summation of $W(E \to E')$ over all the states with energy E' lower than E is equal to the overall transfer rate $W_{\mathrm{tr}}(E)$ which depends on E. Since excitons are localized they can hardly reach impurity and defect centers. We therefore assume that at a given photon energy, E, the excitonic density only decays either through radiative recombination with time T_{r} or through transfer to lower-energy localized states with time $T_{\mathrm{tr}}(E) = W_{\mathrm{tr}}^{-1}(E)$. Other nonradiative decay channels are neglected. Owing to the shrinkage of the exciton center-of-mass wave function with increasing localization energy, the radiative lifetime is expected to increase with localization energy [4, 9]. However, in our case the experimental data concern a rather narrow energy range of about 20 meV and we assume that the energy dependence of the nonradiative decay time due to transfer is much more important than the energy dependence of the radiative one. The radiative decay time, T_r, is then chosen independent of energy.

The transfer probability $W_{tr}(E)$ is taken proportional to the number of states available at lower energy, i.e. $\int_E^\infty g(E')\,dE'$, where the density of states $g(E)$ is chosen proportional to $\exp(-E/E_0)$ (E is the localization energy). A more rigorous expression would be $\exp(-(E/E_0)^n)$, where the exponent n is itself a function of the energy and may vary between 0.5 and 2 [10, 11]. However, owing to the narrow energy range under consideration the exponential approximation is sufficient. As a consequence, the transfer probability $W_{tr}(E)$ is proportional to $\exp(-E/E_0)$. After Cohen and Sturge, the transfer rate $W(E \to E')$ from energy E to E' is proportional to the exchange interaction $J \sim \exp(-R/a_B)$ (a_B is the exciton Bohr radius), to the exciton–phonon coupling, $G^2(\Delta E)$, and to the density of final states $g(E')$. ΔE is the energy mismatch between initial and final exciton states. Since energy and spatial position are supposed to be uncorrelated, the spatial dependence of the transition probability given by $\exp(-R/a_B)$ is eliminated by integration over space. We then obtain $W(E \to E') \sim$ $\sim G^2(\Delta E)\, g(E')$. Since we choose $g(E)$ as $\exp(-E/E_0)$ the transfer probability can be written as

$$w(E \to E') = W_{tr}(E) \frac{G^2(\Delta E)\, g(\Delta E)}{\sum\limits_{\Delta E} G^2(\Delta E)\, g(\Delta E)}\,.$$

Cohen and Sturge considered both piezoelectric and deformation potential coupling, $G_P^2(E)$ and $G_D^2(E)$, and weighted both of them differently according to the alloy concentration. In Fig. 1, curves a and b the energy dependence of $G_P^2(\Delta E)$ and $G_D^2(\Delta E)$ is plotted for the concentration $x = 0.64$ using the same parameters as in [2]. Here the two curves are drawn with their respective intensities as given by the theoretical calculation. One can notice that piezoelectric interaction is much stronger than deformation potential coupling, but that the latter extends over a larger energy range. The total exciton–phonon coupling $G^2(\Delta E)$ is the sum of the two contributions $G_P^2(\Delta E)$ and $G_D^2(\Delta E)$. The product $G^2(\Delta E)\, g(\Delta E)$ presented in Fig. 1, curve c shows the energy range for efficient transfer.

2.2 Experimental results

Luminescence is excited by a picosecond dye laser synchronously pumped by an argon ion laser. TRL is detected through a spectrometer by a synchroscan streak camera. The time resolution is about 50 ps.The experimental setup is described elsewhere [8]. Experiments are performed at pumped liquid helium temperature. Fig. 2 shows the lifetime of localized excitons across the LE band obtained under quasi-resonant excitation. Hereafter, for the sake of simplicity, we neglect the fact that the decay is not strictly exponential on the high-energy side of the LE band. The decay curves are approximated by exponentials for early times [8].

Three parameters are used to fit the experimental lifetime: the characteristic energy, E_0, for the density of states, the radiative lifetime, T_r, and some definite energy, E_{me}, for which the radiative time equals the transfer one. According to Oueslati et al. [12] E_{me} plays a role analogous to a mobility edge although it is by no means related to any change from extended to localized states. The overall decay rate is $T(E)^{-1} =$ $= T_r^{-1}(1 + \exp((E - E_{me})/E_0))$. The best fit gives E_0 in the range 1.8 to 2.5 meV. From lifetime measurements on the low-energy side of the LE band, where recombination is mainly radiative, one finds a radiative lifetime of about 1.1 to 1.2 ns. E_{me} is about 8 meV below the free exciton energy estimated from the positions of the maxi-

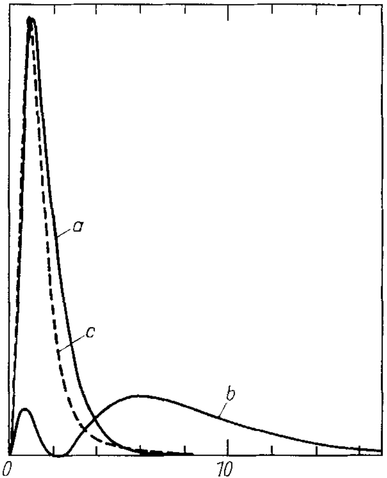

Fig. 1

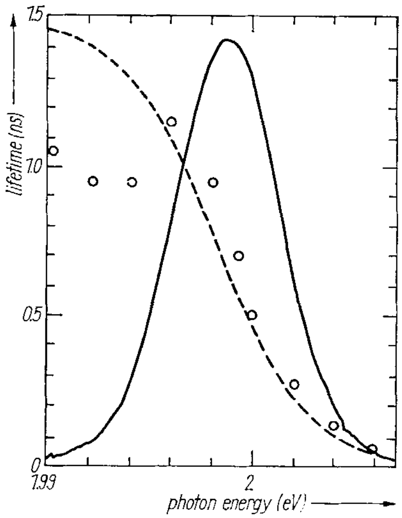

Fig. 2

Fig. 1. Exciton–phonon interaction. (a) Piezoelectric coupling $G_P^2(\Delta E)$, (b) deformation potential coupling $G_D^2(\Delta E)$, where ΔE is the phonon energy equal to the energy mismatch between initial and final exciton states. The parameters of [2] are used in the calculation. The energy scale is expanded by a factor 1.5 (see text). (c) $G^2(\Delta E)\, g(\Delta E)$, where $G^2(\Delta E) = G_P^2(\Delta E) + G_D^2(\Delta E)$ is the total exciton–phonon coupling and the density of states $g(E)$ equals $(1/E_0) \exp(-E/E_0)$ with $E_0 = 2.2$ meV

Fig. 2. Lifetime of localized excitons of $CdS_{0.36}Se_{0.64}$ under quasi-resonant excitation. Whenever the decay curve is not strictly exponential it is approximated at short times by the closest exponential function. The solid curve is the LE luminescence spectrum for above-band-gap excitation. The dashed line is a fit using $T(E)^{-1} = T_r^{-1}(1 + \exp((E - E_{me})/E_0))$ with $E_0 = 2.2$ meV, $T_r = 1.5$ ns, $E_{me} = 1.9982$ eV, ○ experimental points

mum and minimum in the reflectivity spectrum. E_{me} lies in the range 1.998 to 1.999 eV.

The experimental luminescence decay curves are obtained from observations at various photon energies and excitation either in the LE band (Fig. 3a) or at higher energy around the $A_{n=2}$ free exciton energy (Fig. 4a). TRL spectra in Fig. 5 are derived from these data. Fig. 5a and d show the experimental spectra at various delays after the exciting pulse. One can notice the broadening of the band and the shift of its maximum to low energies as time elapses. Finally, Fig. 6 shows time-integrated luminescence spectra under excitation in the LE (parts a, b, and e) and at higher energy (parts c and f). In our calculation luminescence intensity is proportional to the excitonic density. No reabsorption effect is taken into account. We obtain a satisfactory agreement between the above theoretical model and the experimental curves using the following parameters: $E_0 = 2.2$ meV, $T_r = 1.5$ ns, $E_{me} = 1.9982$ eV. It is worthwhile underlining that although the radiative lifetime is only 1.5 ns, luminescence decay curves show a rise time of 2 or 3 ns for large detunings between excitation and observation energies (Fig. 3 and 4). This is entirely due to transfer between localized states. The shorter the energy transfer range, the longer is the rise time of luminescence for a large detuning.

In order to obtain a satisfactory fit for TRL spectra and decay curves at early times we need a wider energy range for the transfer probability than the one given

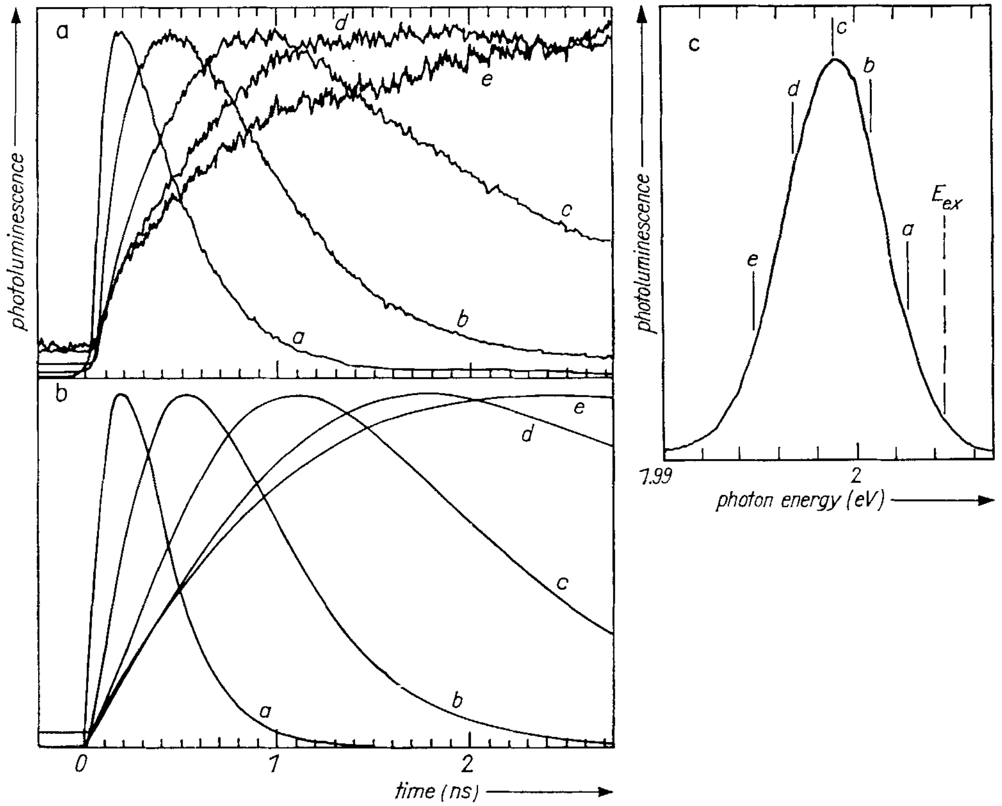

Fig. 3. Luminescence time decay under selective excitation at 2.004 eV. a) Experimental results, b) theoretical results using the model of [2] (see text), c) the excitation energy and the observation energies at (a) 2.0024, (b) 2.0005, (c) 1.9985, (d) 1.9965, (e) 1.9946 eV, respectively

by $G^2(\Delta E)\, g(\Delta E)$. This is achieved by arbitrarily multiplying the energy scale by 1.5 for exciton–phonon interaction. This broadened exciton–phonon coupling was also used by Permogorov et al. to fit time integrated luminescence spectra [3]. We shall comment on this in the next section.

The agreement between experimental and theoretical TRL spectra is better for selective excitation in the LE band than for high energy excitation (Fig. 5 a, b, and d, e). In the first case the initial excitonic density is taken as a δ-like function. In the second case, the initial population is not well known. We assume very fast exciton relaxation down to the bottom of the band and take an initial excitonic density proportional to $(\exp(-E/E_0) - \exp(-E/E_1))$ with the energy origin at 2.006 eV and the parameters E_0 and E_1 equal to 2.2 and 1 meV, respectively. The origin of the energy roughly corresponds to the free exciton energy estimated from the reflectivity maximum and minimum at 2.0059 and 2.0113 eV, respectively. This initial excitonic density is chosen similar to the experimental TRL spectrum at 100 ps (Fig. 6d).

Let us note that both experimental and theoretical decay curves differ from the true decay curves. Due to the sinusoidal sweeping signal applied to the streak camera deflection plates, a luminescence signal occurring at time $t_1 - t$ (where t_1 is about 9 ns in our case) is added to the one observed at time t in the time window $0 < t <$

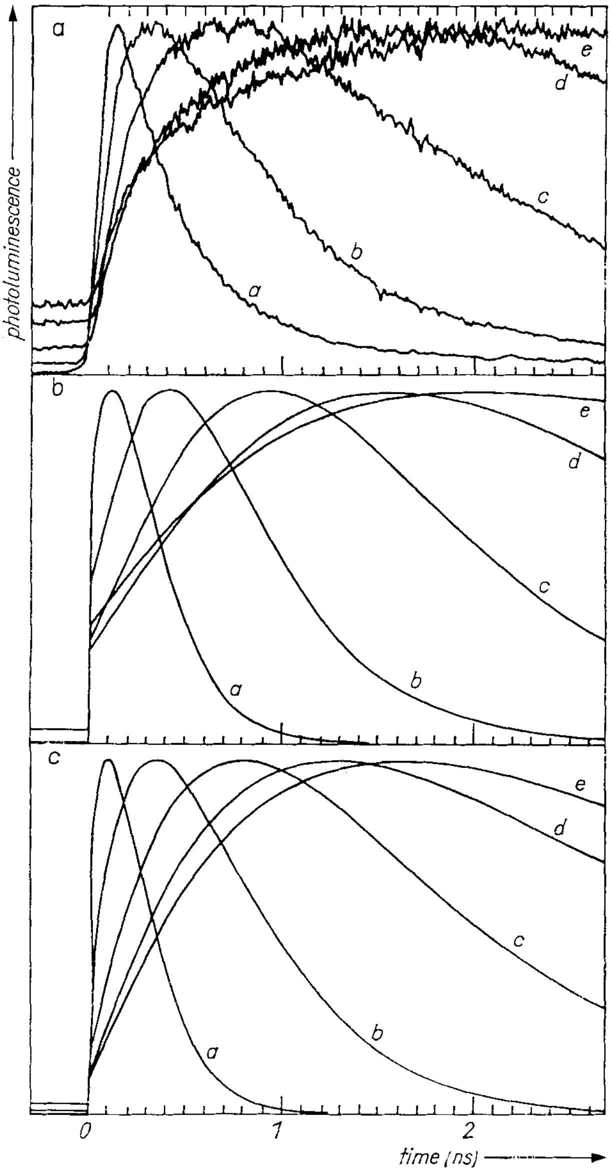

Fig. 4. Luminescence time decay under excitation at 2.0227 eV. a) Experimental results, b) and c) theoretical results using the models of [2] and [12], respectively. The observation photon energies are the same as in Fig. 3

< 3 ns [13]. This effect gives rise to a nonzero intensity before time $t = 0$ and can be observed in Fig. 3a and 4a.

3. Discussion

The kinetics of localized excitons in semiconductor alloys has often been described in a qualitative way because, to our knowledge, no accurate and satisfactory description of localized excitons in semiconductor alloys is available. Several expressions for the density of localized states of electrons or holes have been proposed depending on which

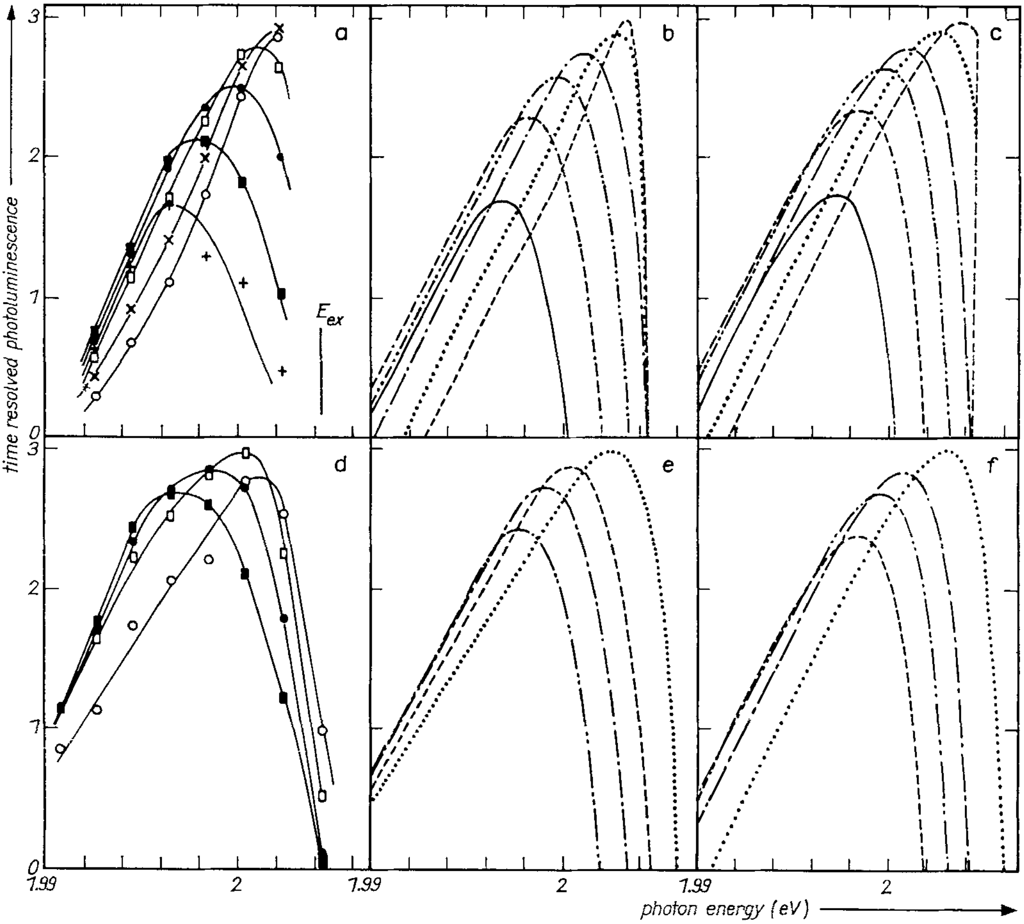

Fig. 5. Time resolved luminescence spectra in logarithmic scale. Upper curves: 100 (○, — — —), 200 (×, ··········), 500 ps (□, ·—·—·), 1 (●, —··—), 2 (■, —·—), and 4 ns (+, ———) time delay after selective excitation at 2.0044 eV; lower curves: 100 (○, ··········), 500 ps (□, — — —), 1 (●, ·—·—·), 2 ns (■, —··—) time delay after excitation at 2.0227 eV; a) and d) experimental results; b) and e) theoretical results using the model of [2]; c) and f) theoretical results using the model of [12]

kind of atomic potential is considered [10]. As for excitons, the density of states is difficult to obtain theoretically [11]. In order to calculate the effect of alloy potential fluctuations on the electron and the hole, both conduction and valence band offsets between the two pure compounds must be well known (which is not the case for $CdS_{1-x}Se_x$). Furthermore the calculation is difficult to carry out unless the localization energy is small compared to the binding energy. In the general case, localization may produce a shrinkage of the exciton Bohr radius as well as a decrease of the spatial extent of the center-of-mass wave function. As a consequence the interaction between localized excitons and acoustic phonons is not known with accuracy.

(i) Although localized excitons were considered so far, the exciton–phonon interaction matrix element was calculated using a plane wave for the center-of-mass wave

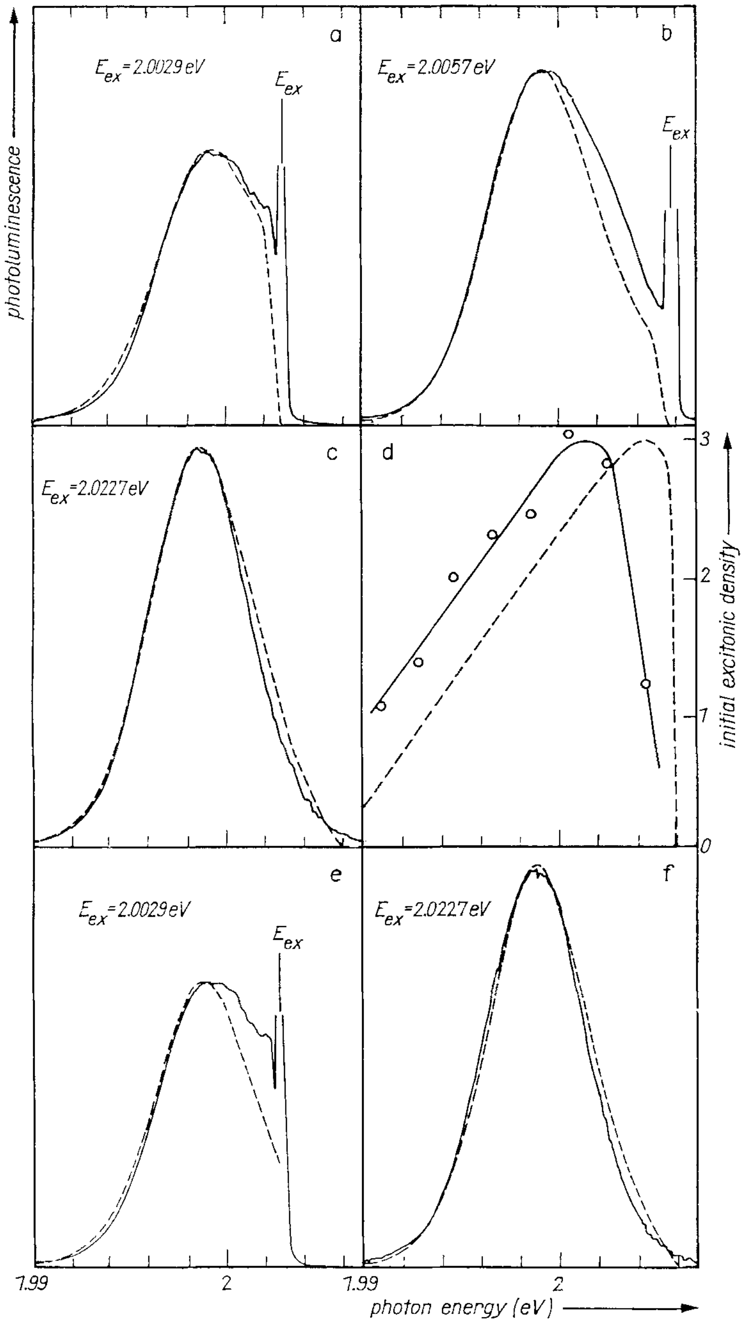

Fig. 6. Time integrated luminescence spectra of $CdS_{0.36}Se_{0.64}$. Solid line: experimental spectrum, dashed line: theoretical fit. For a), b), and c) the theoretical curve is calculated using the model of [2]. For e) and f) the theoretical curve is calculated using the model of [12]. In d) the dashed curve represents the initial excitonic density in logarithmic scale under excitation at 2.0227 eV; the solid curve is the experimental luminescence spectrum at 100 ps

function as in case of free excitons. It would be interesting to use a localized wave function with an energy dependent spatial extension. This would require a good knowledge of the localized exciton wave function.

(ii) Many parameters for CdS and CdSe must be used in the calculation of exciton–phonon interaction. Different values for exciton Bohr radius and hole masses can be found in the literature depending on the choice of the dielectric constant (importance of the polaron effect) and on the assumed value for exciton binding energy [14]. This may strongly influence the respective strength of piezoelectric and deformation potential coupling. For example, arbitrarily decreasing the exciton Bohr radius leads to a decrease of piezoelectric coupling and to an increase of deformation potential coupling. Furthermore, as was noticed in [2], deformation potential values E_c and E_v are not well known.

In view of the above remarks the expansion by a factor 1.5 of exciton–phonon coupling may be justified. It takes into account in a phenomenological way all the above uncertainties and approximations. Contrary to Cohen and Sturge who consider only piezoelectric coupling for alloy compositions close to CdSe, we find it necessary to take into account deformation potential coupling, too. The transfer probability then shows a weak tail. That enables us to obtain a sufficiently fast rise time for the decay curves corresponding to a large detuning from the exciton energy (Fig. 3b and 4b).

In [2] and [3] only piezoelectric coupling is taken into account and TIL spectra are fitted in the energy region where the energy dependent transfer time becomes negligible compared to the radiative lifetime. One can then easily notice that the characteristic energy E_0 describing the density of localized states has no effect as soon as it becomes larger than the characteristic energy for piezoelectric coupling. When one also takes into account deformation potential interaction, increasing E_0 leads to an increased contribution of long-range transfer. The effect of E_0 is even more easily seen on TIL spectra since their widths depend directly on this parameter. Nevertheless we cannot allow E_0 to vary over a wide range since it is deduced from our lifetime measurement.

The spectral position of the TIL spectra depends on E_{me}. In order to obtain the best fit for these spectra we chose $E_{me} = 1.9982$ eV. A slightly larger value would give a better fit with the experimental lifetimes (Fig. 2). This small discrepancy can be explained in the following way. The lifetimes were measured under quasi-resonant excitation, that is 0.2 to 0.3 nm below the excitation wavelength. When the transfer is very fast, one measures the lifetime of excitons which have already transferred and consequently exhibit a larger decay time.

In order to obtain a good agreement with luminescence decay curves at long times we must use a value of 1.5 ns for the radiative decay time though from experimental measurements one would expect it to lie in the range 1.1 to 1.2 ns. We have no satisfactory explanation for this discrepancy.

As already mentioned above, we have approximated the decay behaviour under selective excitation by an exponential function for the whole energy range under consideration. Therefore, we cannot expect a good agreement with experimental results for long times. As a matter of fact, we only obtain a satisfactory fit in a 4 ns range after excitation. The magnitude of the signal appearing before time $t = 0$, which is due to some signal at $t > 9$ ns, is not correctly fitted within this model as one can see in Fig. 3 and 4.

Luminescence assisted by acoustic phonons as well as absorption through the acoustic wing is not taken into account in the model of [2]. This process was proposed by Permogorov et al. [3] to explain the luminescence lineshape under selective excita-

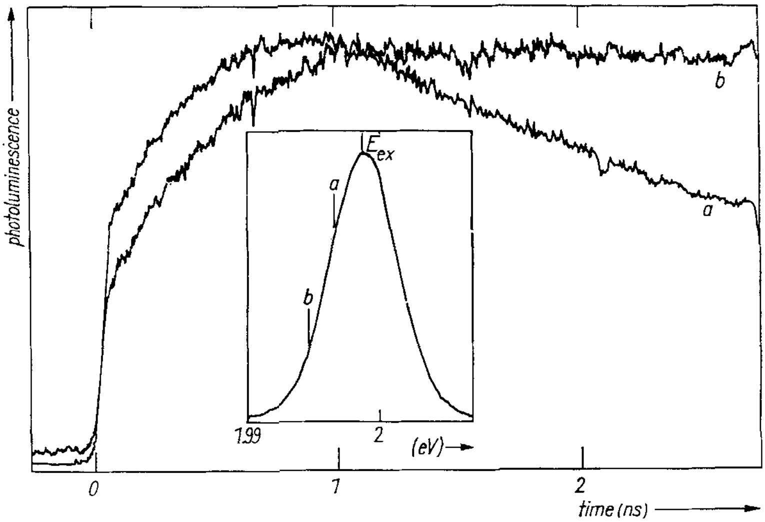

Fig. 7. Luminescence time decay under selective excitation at 1.9993 eV. The inset shows the excitation and observation energies

tion deep in the band tail. In this spectral region, exciton transfer becomes less probable due to the low density of states. Absorption and subsequent luminescence assisted by acoustic phonons become the dominant process with decreasing excitation energy and give rise to a quasi-instantaneous (with our resolution) rise time of the luminescence signal (Fig. 7). In order to reproduce this feature one should take into account a nonzero initial excitonic density and the instantaneous appearance of luminescence signal at energies lower than the excitation one. One must notice that both the transfer model proposed by Cohen and Sturge and the model proposed by Permogorov et al. were utilized to fit similar experimental data. In our opinion fitting only TIL spectra obtained under excitation deep in the band tail is not sufficient to decide which process is the correct one. TRL spectra show that the two processes have to be considered.

4. Comparison with Other Models

In order to describe exciton transfer between localized states in $GaAs_{1-x}P_x$ alloys, Oueslati et al. have introduced a model which involves phenomenological parameters and does not refer to any precise microscopic process. The excitonic density of states obeys the rate equation (1). The only assumption is that the transfer rate $W(E \to E')$ is proportional to the density of final states $g(E')$. Energy conservation is not explicitly taken into account. Neither is any spatial transfer. Two characteristic energies are involved, E_1 and E_0. E_1^{-1} (α in [12]) is the slope of the transfer rate $W_{tr}(E)$ as a function of photon energy in a logarithmic scale: $W_{tr}(E) = T_r^{-1} \exp\left((E - E_{me})/E_1\right)$. Since $W(E < E')$ is proportional to $g(E')$ and the summation over all the energies $E' > E$ is equal to the transfer rate $W_{tr}(E)$, there is an implicit dependence of $W(E \to E')$ on E_1,

$$W(E \to E') = \frac{1}{T_r E_0} \exp\left(\frac{E_{me}}{E_1}\right) \exp\left[-E\left(\frac{1}{E_1} - \frac{1}{E_0}\right)\right] \exp\left(-\frac{E'}{E_0}\right), \qquad (2)$$

where E and E' are localization energies.

Theoretical curves are presented in Fig. 4c, 5c, 5f, 6e, and 6f. We obtain a satisfactory fit with $E_0 = 1.5$ meV, $E_1 = 1.8$ meV, $T_r = 1.5$ ns, $E_{me} = 1.9986$ eV. Let us note that $E_1 > E_0$. It means that for a fixed E', the transfer rate $W(E \rightarrow E')$ increases with increasing E. Thus transfer with small energy detuning is more probable. When $E_1 < E_0$, as in [12], the transfer rate increases with decreasing E. This can also be explained if one neglects energy conservation but considers spatial transfer. Transfer by the tunnel effect is more likely to occur from those states because they have a broad spatial extension [15].

The values of the parameters are close to those found with the previous model. However, for a selective excitation in the LE band, transfer to excitonic states within a short-energy range is more accurately described with the model of Cohen and Sturge. This can be seen in TRL spectra (Fig. 5 a, b, c) and TIL spectra (Fig. 6 a, e). This good agreement is due to the fact that the energy dependence of the exciton–phonon interaction (mainly piezoelectric coupling) is explicitly taken into account (see Fig. 1).

In the model presented by Shevel et al. [6] microscopic processes are considered. Spatial transfer is taken into account through the tunnel effect between localized states but energy conservation is discarded. The only energy dependence of the transfer rate comes from the number of states available at lower energy. The model leads to nonexponential decays for selectively excited states in the LE band ((7) of [6]). The process is very similar to donor–acceptor recombination. Under quasi-resonant excitation on the high-energy side of the LE line we could indeed observe this nonexponential decay [8]. However, the dynamic range was not sufficient to fit accurately the data with a nonexponential function. For above-band-gap excitation relaxation from higher energy states tends to blur the effect of spatial transfer because many intermediate states are involved in the process. The long rising time of the luminescence intensity prevents one from precisely measuring the decay time of the states under consideration. In [6] Shevel et al. discuss a short time approximation of their model. In this approximation spatial transfer is neglected and the model becomes equivalent to the short time limit of the model developed by Oueslati et al. when $E_1 = E_0$. The limitation in time domain seems to be stringent since it requires $t < \nu_0^{-1}$ where $\nu_0 \approx 10^{11}\ s^{-1}$ is the attempt-to-escape frequency. Although the time range under consideration is much larger than ν_0^{-1}, we tried a fit of our data for above-band-gap excitation with Shevel et al.'s model in this approximation ((9) of [6]). We find a rather satisfactory agreement using $E_0 = 2.2$ meV, $T_r = 1.5$ ns, $E_{me} = 1.9986$ eV (the parameter g of [6] is then equal to 100 ps). We conclude that it is difficult to clearly demonstrate the influence of spatial transfer on luminescence time decay when the dynamic range is small and the system under study involves many relaxation stages.

5. Conclusion

We applied the model formerly developed by Cohen and Sturge describing transfer between localized exciton states in $CdS_{1-x}Se_x$ by a tunnel effect assisted by acoustic phonons. We obtain a satisfactory agreement with time decay curves, time resolved luminescence spectra, and time integrated luminescence spectra. We underline the following point. Whereas it is rather easy to obtain a good fit with time integrated luminescence spectra on a linear scale, it is much more difficult to concurrently fit TIL spectra, time decay curves, and TRL spectra on a logarithmic scale. Let us also note that some information is lost when each decay curve is normalized to its maximum. On the other hand, TRL spectra derived from the decay curves contain all the available information on the system.

We used the exciton–phonon interaction parameters of [2]. From the best fit of experimental curves we find the radiative lifetime equal to 1.5 ns and the characteristic energy for the band tail density of states is equal to 2.2 meV. The energy range for one-step efficient energy transfer between localized states is of the order of a few meV. We also considered the model of Oueslati et al. Although this model involves only a small set of parameters, two of which, E_1 and E_{me}, are phenomenological ones, it enables us to obtain a good fit of our experimental results. This is highly valuable in view of the complexity of the localized excitons system.

References

[1] S. Permogorov and A. Reznitskii, Proc. Internat. Conf. Excitons 84, Güstrow (DDR), Pädagogische Hochschule Güstrow, 1984 (p. 194).
[2] E. Cohen and M. Sturge, Phys. Rev. B **25**, 3828 (1982).
[3] S. Permogorov, A. Reznitskii, S. Verbin, G. O. Müller, P. Flögel, and M. Nikiforova, phys. stat. sol. (b) **113**, 589 (1982).
[4] S. Permogorov, A. N. Reznitskii, S. Yu. Verbin, and V. A. Bonch-Bruevich, Zh. eksper. teor. Fiz., Pisma **38**, 22 (1983).
[5] J. A. Kash, A. Ron, and E. Cohen, Phys. Rev. B **28**, 6147 (1983).
[6] S. Shevel, R. Fisher, E. O. Göbel, G. Noll, and P. Thomas, J. Lum. **37**, 45 (1987).
[7] Ya. Aaviksoo, Ya. Lippmaa, S. Permogorov, A. Reznitskii, P. Lavallard, and C. Gourdon, Zh. eksper. teor. Fiz., Pisma **45**, 391 (1987).
[8] C. Gourdon, P. Lavallard, S. Permogorov, and A. Reznitsky, J. Lum. **39**, 111 (1987).
[9] E. I. Rashba and G. E. Gurgenishvili, Fiz. tverd. Tela **4**, 1029 (1962).
[10] B. I. Halperin and M. Lax, Phys. Rev. **148**, 722 (1966).
W. Sritrakool, V. Sayakanit, and H. R. Glyde, Phys. Rev. B **33**, 1199 (1986).
[11] S. D. Baranovskii and A. L. Efros, Fiz. Tekh. Poluprov. **2**, 2237 (1978).
[12] M. Oueslati, C. Benoit à la Guillaume, and M. Zouaghi, Phys. Rev. B **37**, 3037 (1988).
[13] P. Geist, F. Heisel, A. Martz, and J. A. Miehé, Rev. Phys. appl. **19**, 619 (1984).
[14] J. J. Hopfield and D. G. Thomas, Phys. Rev. **122**, 35 (1961).
J. Voigt, F. Spiegelberg, and M. Senoner, phys. stat. sol. (b) **91**, 189 (1979).
R. G. Wheeler and J. O. Dimmock, Phys. Rev. **125**, 1805 (1962).
B. Segall and D. T. F. Marple, in: Physics and Chemistry of II–VI Compounds, Ed. M. Aven and J. S. Prener, North-Holland Publ. Co., Amsterdam 1967 (p. 344).
[15] C. Benoit à la Guillaume, private communication.

(Received February 8, 1989)